Food & Function

ROYAL SOCIETY OF CHEMISTRY

PAPER

View Article Online
View Journal | View Issue

Cite this: *Food Funct.*, 2023, **14**, 8814

Effect of nano-encapsulated food flavorings on streptozotocin-induced diabetic rats

Dina Mostafa Mohammed, *[a] Mohamed A. Abdelgawad,[b] Mohammed M. Ghoneim,[c,d] Mohamed El-Sherbiny,[e,f] Wael A. Mahdi,[g] Sultan Alshehri, [g] Hasnaa A. Ebrahim[h] and Amr Farouk[i]

Flavors and aromas are widely used in food and pharmaceutical industries to enhance food palatability. However, it is worth noting that they may also have bioactivity. This study aims to examine the potential impact of key flavors and their nanocapsules on health and diseases, such as type 2 diabetes mellitus (T2DM). The 36 nanocapsules of key flavorings were prepared by high shear homogenization (HSH). Seventy-two male Sprague-Dawley rats received a single dosage of streptozotocin (35 mg kg^{-1} body weight) intraperitoneally. All of the nutritional and biochemical parameters were statistically analyzed. A virtual docking study was conducted. Linalool nanoemulsion results showed the highest encapsulation efficiency (86.76%), while isoamyl acetate nanoparticles showed the lowest (69.99%). According to GC-MS analysis, encapsulation did not affect the flavoring structure with particle size distributions ranging from 277.3 to 628.8 nm. Using TEM, nanoemulsion particles appeared spherical with a desired nanometric diameter size. In the oral glucose tolerance test, flavorings in oil and nanoforms had no discernible hypoglycemia effects in normal rats. The nutritional and biochemical parameters confirmed that both normal and nanoencapsulation forms demonstrated a potential anti-hyperglycemic effect, and enhanced the rat health compared to the raw flavorings. The studied flavorings and their nanocapsules seem to have the potential double effect of a flavor compound as a food palatability enhancer with a potential beneficial effect on type 2 diabetes mellitus without any health drawbacks.

Received 3rd April 2023,
Accepted 21st August 2023

DOI: 10.1039/d3fo01299a

rsc.li/food-function

1. Introduction

Flavors and aroma are crucial in making food products more appealing to consumers. However, they may also have bioactivity, especially those naturally occurring in fruits and vegetables. For instance, many aroma components of essential oils, such as terpenes and terpenoids, have been proposed to contribute to the antimicrobial include bacteria and fungi, antiviral, anti-inflammatory, analgesic, antioxidant, and many other bioactivities. These include α-terpinene, β-terpinene, and β-terpinolene in tea tree (*M. alternifolia*); 1,8-cineole in *M. aquatica* L., *M. longifolia* L., and *M. piperita* L.; menthone and isomenthone in *M. longifolia* and *M. piperita*; thymol, eugenol, and linalool in black cumin, cinnamon bark, and ginger; thymol; eugenol in thyme and clove leaf; and neral/geranial (citral), citronellal, isomenthone, and menthone in lemon balm oil (*M. officinalis* L.).[1]

The necessity for preventive bioactive ingredients, nutraceuticals, or functional foods as an essential element in the diets of today's cuisine to overcome poor dietary habits and sedentary lifestyles that increase the prevalence of chronic degenerative diseases, such as type 2 diabetes mellitus (T2DM), represents a potential objective.[2] Hyperglycemia, a hallmark of T2DM, involves numerous biological processes, including glucose absorption, insulin resistance, and secretion.[3] More than 537 million people worldwide are diagnosed with T2DM, accompanied by diagnostic complications, such as cardiovascular and neuropathy diseases.[4] The main proteins involved in T2DM and its development are glucagon-like peptide-1, glu-

[a]*Department of Nutrition and Food Sciences, National Research Centre, Dokki, Cairo, 12622, Egypt. E-mail: dina_ganna@yahoo.com; Tel: +201003715090*
[b]*Department of Pharmaceutical Chemistry, College of Pharmacy, Jouf University, Sakaka 72341, Saudi Arabia*
[c]*Department of Pharmacy Practice, College of Pharmacy, AlMaarefa University, Ad Diriyah 13713, Saudi Arabia*
[d]*Pharmacognosy and Medicinal Plants Department, Faculty of Pharmacy, Al-Azhar University, Cairo 11884, Egypt*
[e]*Department of Basic Medical Sciences, College of Medicine, AlMaarefa University, Riyadh 11597, Saudi Arabia*
[f]*Department of Anatomy, Faculty of Medicine, Mansoura University, Mansoura 35516, Egypt*
[g]*Department of Pharmaceutics, College of Pharmacy, King Saud University, Riyadh 11451, Saudi Arabia*
[h]*Department of Basic Medical Sciences, College of Medicine, Princess Nourah bint Abdulrahman University, Riyadh 11671, Saudi Arabia*
[i]*Flavour and Aroma Chemistry Department, National Research Centre, Dokki, Cairo, 12622, Egypt*

tamine fructose-6-phosphate amidotransferase, 17-hydroxysteroid dehydrogenase, dipeptidyl peptidase IV, C-reactive protein, protein tyrosine phosphatases, and insulin-like growth factor 1 receptor kinase.[5]

Many flavorings, such as limonene, citral, and linalool, demonstrated antidiabetic activity.[6–8] However, their nanoforms or their effects on the proteins responsible for T2DM development have not been studied. Nanoencapsulation seems promising for applying different flavorings in various sectors to avoid poor dispersibility in hydrophilic media and susceptibility to environmental conditions.[9] Therefore, the conventional delivery of antidiabetic drugs through encapsulation into a nanoform leads to a thermodynamic therapeutic agent that is stable for a longer time and can overcome difficulties, including insufficient absorption, inadequate bioavailability, and drug deterioration.[9] Therefore, this work aimed to investigate the impact of crucial food flavorings widely applied in foods and pharmaceuticals; linalool, orange peel oil, citral, isoamyl acetate, and allyl caproate on streptozotocin-induced diabetic rats and find out any drawbacks or developments in T2DM. In addition, the potential antidiabetic properties were investigated using an *in silico* approach by predicting the binding interactions between flavorings and target cell signaling proteins involved in the development of diabetes. The effect of encapsulation into nanoparticles using high shear homogenization (HSH) on T2DM and the flavorings' antidiabetic properties was also studied.

2. Materials and methods

2.1. Materials

The *n*-alkanes C_6–C_{26} mixture, isoamyl acetate (≥97%), linalool (≥97%), citral (≥96%), allyl caproate (≥98%), diethyl ether, sodium sulfate anhydrous, Tween 80, casein, cellulose, and streptozotocin (STZ) were supplied by Sigma-Aldrich (St Louis, MO, USA). Orange peel oil was provided by Ernesto Ventos S.A. (Brazil). Maltodextrin MD with DE 12-15 (National Co. for Corn Products, 10th of Ramadan, Egypt), sodium caseinate (SC) (Fonterra, New Zealand), and gum Arabic (GA) (Avonchem, Cheshire, UK) were the components used for the wall formulations. The unsaturated fat, sucrose and maize starch were supplied from a local market. ELISA kits were purchased from Abcam (Discovery Drive, Cambridge Biomedical Campus, Cambridge, CB2 0AX, UK), and other kits were acquired from the Biodiagnostic Company, Egypt.

2.2. Methods

2.2.1. Preparation of nanoencapsulation for flavorings. The coating solution was prepared using a previously described procedure based on,[10] with some modifications. Briefly, GA (15% weight/volume w/v) and SC (5% w/v) were dissolved t separately in warm deionized water, and kept at 4 °C overnight to enable the polymer molecules to hydrate thoroughly. A total solid content of 35.0% w/v was then achieved by dissolving MD (15% w/v) in the gum solution first, followed by SC, while stirring constantly. The ratio of the core and wall was about 1 : 2 to achieve the best encapsulation efficiency, as reported by[10] with respect to the wall composition.[10,11] After dissolving Tween 80 (1.0% w/v, based on water), flavorings were added to the coating solution to create a 15% w/v water-feeding emulsion. After emulsification for 15 min with a magnetic stirrer (Bibby Scientific Ltd, U.K., 230 V, 500 W, 50 Hz), the mixture was homogenized using a high-speed homogenizer (PRO 400 PC, Pro Scientific, USA) at 20 000 rpm for 20 min in an ice bath to reduce the temperature to less than 5 °C.

2.2.2. Effect of the encapsulation process on the chemical structure of flavorings and orange oil. The effect of the encapsulation technique applied during the study was investigated by gas chromatographic-mass spectrometry (GC-MS) analysis. Following,[11] a vortex mixer combined 2 ml of flavoring nanocapsules in a screw-cap vial mixed with 4 ml of diethyl ether. After settling and drying using anhydrous sodium sulfate, the supernatant was transferred to a 2 mL screw-cap vial that was wrapped with aluminum foil at 20 °C until analysis. The orange peel oil was extracted from the nanocapsules using the Clevenger distillation process.[10] All extraction steps were repeated in triplicate.

2.2.3. Nanoparticle measurement techniques

2.2.3.1. Nanoemulsion characterizations. The particle size distribution, polydispersity index (PDI) and ξ-potential were estimated *via* Zeta Sizer Nano ZS (Nano-S90, Zetasizer, MalvernPanalytical Ltd, Enigma Business Park, Grovewood Road, United Kingdom) at 25 ± 0.1 °C.[12] The sample was prepared by diluting an adequate volume of emulsion sample of about 0.1 ml, which was added to about 3.5 ml of distilled water. Then, the mixture was subjected to gentle sonication. The diluted sample was transferred to a 3 ml disposal PVC transparent cuvette, where 1 ml was used for measurements. For each sample, a detection angle of 173 °C was chosen for the size measurement. The formula for calculating the encapsulation efficiency was encapsulation (%) = $W_s/W_t \times 100\%$, where W_s and W_t are the amounts of the supernatant and total flavoring, respectively. The nanoemulsion was mixed with diethyl ether using a vortex, and then ultrasonically processed for 30 minutes at 37 °C before Gas Chromatography-Mass Spectrometry analysis.[13]

Transmission electron microscopy was used to determine the morphology of the nanocapsules and nanoemulsions (JED 1230, JEOL Ltd, and Tokyo, Japan). A 200-mesh copper specimen grid was coated with 20 microliters of the diluted sample, which was then left for 10 minutes while the extra liquid was blotted away using filter paper. Following one drop of 3% phosphotungstic acid staining, the grids were left to dry for three minutes. After drying, the coated grids were observed under a TEM microscope. The samples were examined *via* 160 kV operation.[14]

2.2.3.2. Gas chromatography-mass spectrometry (GC-MS) analysis

Analysis was performed using a GC (Hewlett-Packard model 5890) connected to an MS (Hewlett-Packard model 5970).

Volatiles were separated on DB-5 (60 m × 0.32 mm × 0.25 mm film thickness, J & W Sci., USA). The oven was kept at 50 °C for the first five minutes, and then scheduled to increase by 4 °C per minute from 50 to 250 °C. The flow rate of the helium carrier gas was 1.1 ml min^{-1}. The split ratio was 1 : 10, the injector temperature was 220 °C, and the sample volume was 2 μL. At 70 eV, electron impact mode (EI) mass spectra were obtained, with the scan *m*/*z* ranging from 29 to 400 amu. Calculating the retention indices of the isolated volatile molecules included using the retention times of the *n*-alkanes series (C_6–C_{22}), which were performed under identical circumstances. Published data, standards, and mass spectrum databases (National Institute of Standards and Technology, NIST) were used to identify the isolated peak.[15]

2.2.4. The biological evaluation of experimental animals

2.2.4.1. Animal study. Seventy-two male Sprague-Dawley rats averaging 150–200 g and aged 2 months were sourced from the Animal House Colony of the National Research Center in Cairo, Egypt. Before the experiment, the animals were given a standard laboratory diet of food and water for a week to help them to acclimate and confirm appropriate development and behavior. Solid-bottomed cages were used to distribute and house the animals in a clean, temperature-controlled (23 °C), relative humidity-controlled (40–60%), and artificially lit (12 h dark/light cycle) room. The Ethical Committee of Medical Research approved the animal study protocol at the Egyptian National Research Centre (Approval no. 1495062022). All animals were handled humanely, and used in accordance with the national law and the UK's Animals (Scientific Procedures) Act, 1986 and its supporting guidelines, as well as EU Directive 2010/63/EU for animal research (Publication No. 85-23, revised 1985).

2.2.4.2. Diet composition. The synthetic base diet was formulated with modification using casein (150 g kg^{-1} diet), unsaturated fat (100 g kg^{-1} diet), sucrose (220 g kg^{-1} diet), maize starch (440 g kg^{-1} diet), cellulose (40 g kg^{-1} diet), salt mixture (40 g kg^{-1} diet), and vitamin mixture (10 g kg^{-1} diet), as stated by.[16,17] The AIN-93M diet was a reference for formulating the salt and vitamin mixtures.[18]

2.2.4.3. Diabetes induction. A single STZ dosage for inducing diabetes (35 mg per kg BW) was diluted in 50 mM citrate buffer pH 4.5.[8] The diabetic rats' blood glucose levels were tracked for two days after they received STZ intraperitoneally on the first day of the trial.[19]

2.2.4.4. Experimental design. Seventy-two rats were organized into (12) groups of six, each of which was characterized as follows:

- Negative control: Normal rats received a synthetic base diet.
- Positive control: STZ-induced diabetic rats received a synthetic base diet.
- Group (1): Diabetic rats received a synthetic base diet supplemented with an oral daily dose of citral (45 mg per kg BW per day).[8]
- Group (2): Diabetic rats received a synthetic base diet supplemented with an oral daily dose of nano-encapsulated citral (45 mg per kg BW per day).[8]
- Group (3): Diabetic rats received a synthetic base diet supplemented with an oral daily dose of linalool (25 mg per kg BW per day).[20]
- Group (4): Diabetic rats received a synthetic base diet supplemented with an oral daily dose of nano-encapsulated linalool (25 mg kg per BW per day).[20]
- Group (5): Diabetic rats received a synthetic base diet supplemented with an oral daily dose of allyl caproate (100 mg per kg BW per day).[21]
- Group (6): Diabetic rats received a synthetic base diet supplemented with an oral daily dose of nano-encapsulated allyl caproate (100 mg per kg BW per day).[21]
- Group (7): Diabetic rats received a synthetic base diet supplemented with an oral daily dose of isoamyl acetate (10 mg per kg BW per day).[22,23]
- Group (8): Diabetic rats received a synthetic base diet supplemented with an oral daily dose of nano-encapsulated isoamyl acetate (10 mg per kg BW per day).[22,23]
- Group (9): Diabetic rats received a synthetic base diet supplemented with an oral daily dose of orange peel oil (600 mg per kg BW per day).[24]
- Group (10): Diabetic rats received a synthetic base diet supplemented with an oral daily dose of nano-encapsulated orange peel oil (600 mg per kg BW per day).[24]

2.2.4.5. Oral glucose tolerance test (OGTT). The rats' glucose tolerance was assessed using the OGTT. On normal rats that had fasted the night before, the OGTT was conducted. Rats were given Glibenclamide (2 mg kg^{-1}) and food flavorings (citral, linalool, allyl caproate, isoamyl acetate, and orange oil). After pretreatment with distilled water, Glibenclamide, and the flavorings individually in both conventional and nano-encapsulated forms, glucose (2 g kg^{-1}) was administered 30 minutes later. Then, blood glucose levels were assessed using heparinized capillary tubes at 0, 30, 60, and 120 minutes. A glucometer and glucose test strips were used to measure the blood sugar.

2.2.4.6. Blood sample collection. After the two-month study period, the animals were fasted for 12 hours and then anesthetized with ketamine hydrochloride (35 mg kg^{-1} i.m.) before being sacrificed by cervical dislocation. The serum and plasma were separated from the blood samples by centrifugation (Sigma Labor Centrifuge GMBH, Germany, model 2-153360 osterode/Hz) at 4000 rpm for 15 minutes, and stored at −20 °C.

2.2.4.7. Biochemical parameters. Insulin, tumor necrosis factor (TNF-α), and interleukin-6 (IL-6) were analyzed by ELISA kits. By using the enzymatic colorimetric technique, glucose,[25] Hb,[26] and the total cholesterol, HDL, LDL, and triglycerides were determined.[27–30] Colorimetric methods were used to assess alkaline phosphatase (ALP), aspartate aminotransferase (AST), and alanine aminotransferase (ALT) activities,[31,32] and total plasma protein and plasma albumin[33,34] as indices of liver function. As indications of renal function, colorimetric methods measured creatinine, urea, and uric acid.[35–37]

2.2.5. Molecular docking.

The crystal structure of glucagon-like peptide-1, human glucose:fructose-6-phosphate ami-

dotransferase, human estrogenic 17β-hydroxysteroid dehydrogenase, the crystal structure of human dipeptidyl peptidase IV, human C-reactive protein, and the crystal structure of PTP1B-inhibitor complex, and insulin-like growth factor 1 receptor kinase (PDB IDs: 3IOL, 2ZJ3, 1BHS, 1J2E, 1GNH, 2NT7 and 1K3A, respectively), originating from the Protein Data Bank (PDB) (**https://www.rcsb.org/**), were accessed on September 22 and 26, 2021 and January 17, 2022. Water, co-crystallized ligands, and ions were removed from receptors, which were subsequently protonated using Pymol software (Ver. 2.5.1). Avogadro Software (Version 1.2.0) was used to improve the ligands' 3D structure retrieved from the PubChem database, accessed on August 4, 2021 (**https://pubchem.ncbi.nlm.nih.gov/**).[38] A web-based application called SwissDock, accessed on September 18, 2021, and January 18–19, 2022 (**https://www.swissdock.ch/docking**), was used to execute blind docking. SwissDock predicts all probable binding sites on a target protein. It operates using a docking program called EADock DSS. Chimera 1.15 software was used to visualize the docking results (ΔG), whereas the best-docked complexes' interface and visualization profiles were created using the Discovery Studio software (Version 21.1.0.20298).[39]

2.2.6. Statistical analysis. The SPSS/PC software (version 22.0; SPSS Inc., Chicago, IL, USA) was used to perform one-way analyses of variance (ANOVA) and *post hoc* multiple comparisons using the Duncan test to evaluate the differences in all biochemical parameters.

3. Results and discussion

3.1. The effect of encapsulation on the flavorings' physicochemical properties

3.1.1. Gas chromatography-mass spectrometry (GC-MS). GC-MS was used to characterize the chemical composition of the flavorings and orange oil nanocapsules compared to their standards. Except for orange oil, the encapsulation technique applied in this study by HSH does not affect the chemical composition of the flavorings used (Fig. 1). The coating compositions chosen in the current study were based on previous findings,[10] which studied the effect of different wall materials in coating other flavorings, and reported that the optimum concentration was MD–GA–SC in the ratio of 15%–15%–5%.

In agreement with,[40] a decrease in the major component, limonene, with the formation and increase in oxygenated terpenes was observed due to encapsulation compared to the control, as shown in Table 1. The capsule's physical stability and biological activity may change due to the formulation using energy-intensive procedures like HSH, which may cause Ostwald ripening, flocculation, or coalescence.[12] Interestingly, non-oxygenated terpene concentrations found in the essential oil decreased as the oxygenated terpene concentrations increased in the oil nanocapsules. As a result, additional research can be done to determine the stability of various volatile substances and essential oils during microencapsulation procedures, particularly under harsh conditions, and to learn

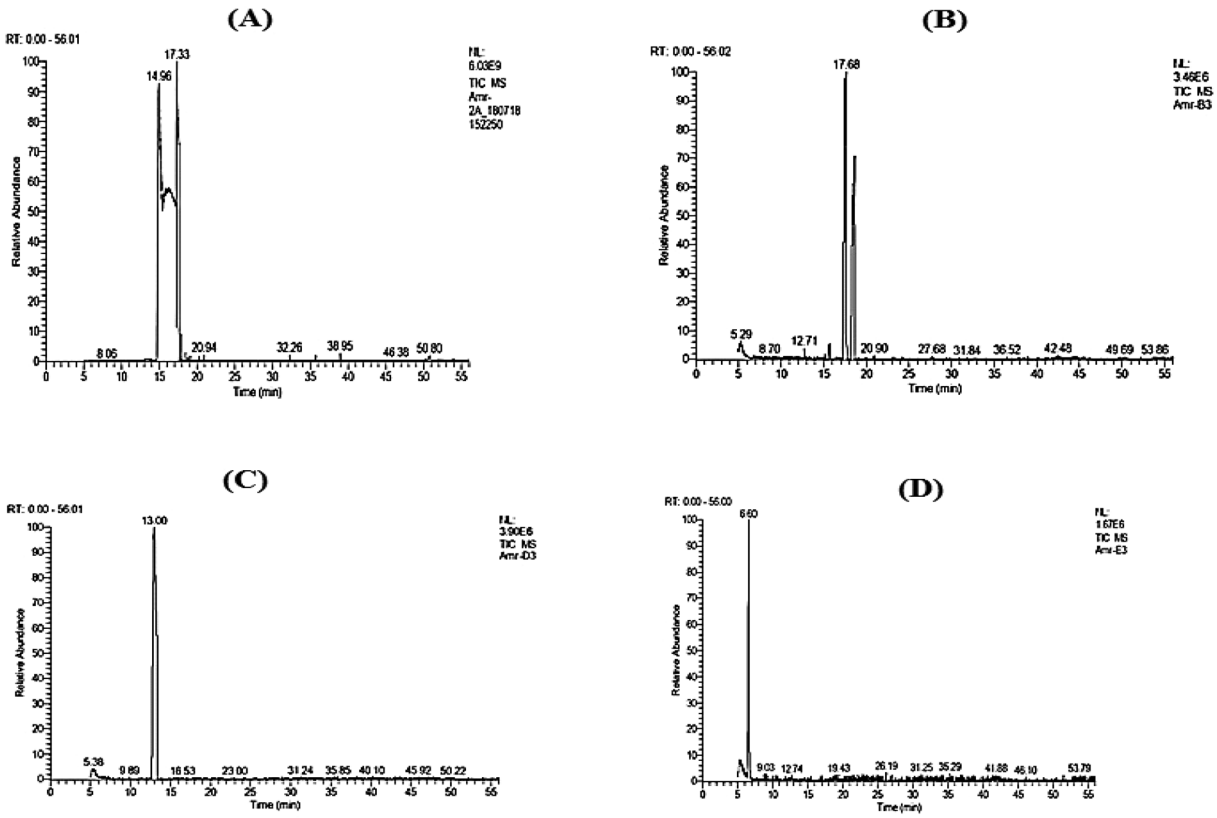

Fig. 1 GC-MS chromatograms of nanocapsules (A) linalool, (B) citral, (C) allyl caproate, and (D) isoamyl acetate.

Table 1 Identification of the volatile constituents of orange peel oil and its nanocapsules using GC-MS

Peak No.	Components	RI[a]	% Area		Method of Identification[b]
			Control	Nanoform	
1	α-Pinene	938	0.44	0.49	RI, MS
2	Sabinene	978	—	0.25	RI, MS
3	α-Myrcene	992	2.13	1.42	RI, MS, STD
4	Limonene	1037	97.43	92.06	RI, MS, STD
5	Linalool	1104	—	0.36	RI, MS
6	*p*-Mentha-2,8-dienol	1129	—	0.8	RI, MS
7	Limonene oxide	1140	—	1.31	RI, MS
8	4-Terpineol	1144	—	0.23	RI, MS
9	*trans*-Carvacrol	1207	—	0.28	RI, MS
10	Linalyl acetate	1253	—	2.62	RI, MS
	Total	—	100	99.99	—

[a] RI: retention indices calculated on DB-5 column using alkanes standards. [b] Confirmed by comparison with the retention indices (RI), the mass spectrum of the authentic compounds (STD), and the NIST mass spectra library data (MS).

the mechanisms of transmitting such volatile substances to others.

Table 1 shows a remarkable decrease in limonene, the major component of the orange peel oil, from 97.43% to 92.06% due to the nanoencapsulation process with the formation of oxygenated terpenes like linalool, limonene oxide, and linalyl acetate.

3.1.2. Droplet size, ξ-potential and polydispersibility index. The DLS technique was used to evaluate the droplet size distribution, zeta potential and PDI of the nanocapsules. All formulated nanocapsules exhibited a monomodal size distribution pattern. Citral and isoamyl acetate showed the smallest *z*-average size for the nanocapsules, 277.3 and 287.1 nm, respectively. In contrast, the orange oil droplets showed the largest *z*-average size (628.8 nm). The particle size increase from citral to allyl caproate, linalool, and orange oil is evidence of micelles swelling to accommodate the solubilized load of extracts. The zeta potential plays a vital role in maintaining the physical stability of emulsions. A higher zeta potential, whether positive or negative, indicates greater stability in the emulsions. According to Table 2, linalool, allyl caproate, and citral showed the highest potential with the smallest PDI and an increase in encapsulation efficiency. The PDI shows the dispersions' uniformity, which ranges between zero and one (Table 2). Molecular weight and vapor pressure are the reasonable and primary factors determining aroma diffusion, where an inverse relationship was observed.[11] The encapsulation efficiency % data showed the highest percentages for the linalool and allyl caproate nanoemulsions compared to other samples, with 86.76 and 86.33%, respectively (Table 2). In contrast, the isoamyl acetate nanoemulsion showed the lowest % among the investigated flavorings (69.99%). This is because it has the lowest molecular weight (130.19 g mol^{-1}) compared to the other investigated flavorings, and the highest vapor pressure (4 mmHg at 20 °C), and the lowest boiling point (142.5 °C).

Table 2 Particle size, PDI, and encapsulation efficiency of nanoemulsions

Nanoemulsion	Particle size (nm)	ξ-Potential (mV)	PDI	Encapsulation efficiency %
Linalool	428.4 ± 19.55	−34.54 ± 1.08	0.290 ± 0.05	86.76 ± 2.28
Citral	277.3 ± 13.34	−26.74 ± 1.79	0.237 ± 0.08	82.36 ± 2.63
Orange peel oil	628.8 ± 25.12	−19.31 ± 1.54	0.487 ± 0.09	83.97 ± 2.02
Allyl caproate	337.3 ± 16.80	−31.25 ± 2.18	0.322 ± 0.06	86.33 ± 1.74
Isoamyl acetate	287.1 ± 17.14	−17.47 ± 1.17	0.394 ± 0.04	69.99 ± 1.65

The drop size distribution of the flavorings is in good agreement with,[41] where MD, WPC, and GA were used to encapsulate red ginseng extract with particle sizes ranging from 100 nm to 3 μm. Also, nano-encapsulated *M. piperita* using chitosan and *Alyssum homolocarpum* gum with a particle size distribution range from 490–790 nm demonstrated that the droplet size distribution is consistent across all samples.[42] The cause for variations in the size of the droplets of various forms can be attributed to variations in the emulsifying capabilities of multiple coatings, surface activity, surface adsorption rate at the droplet level, ductility, and intramolecular interactions in the oil–water joint.[42] The value of close to zero for the PDI index indicates homogeneity in size for the dispersion particles. However, for PDI index values greater than 0.5, non-uniformity in particle size could be observed.[43] Therefore, the formulated nanoparticles shown in Table 2 exhibited good uniformity.

3.1.3. Transmission electron microscopy. TEM is a technique that is frequently used to validate droplet size findings. Image J software was used to adjust the contrast between the background and particles, and automatically determine the diameter of spherical nanoparticles. Fig. 2 demonstrates that the nanoemulsion particles appear dark and spherical with the necessary nanometric diameter size. The TEM and dynamic light scattering results are slightly different since TEM produced a lower value. This is expected, as shrinkage may occur when samples are dried for TEM investigation.[44] The orange oil peel nanoparticles discovered in this investigation had an average diameter larger than similar flavorings

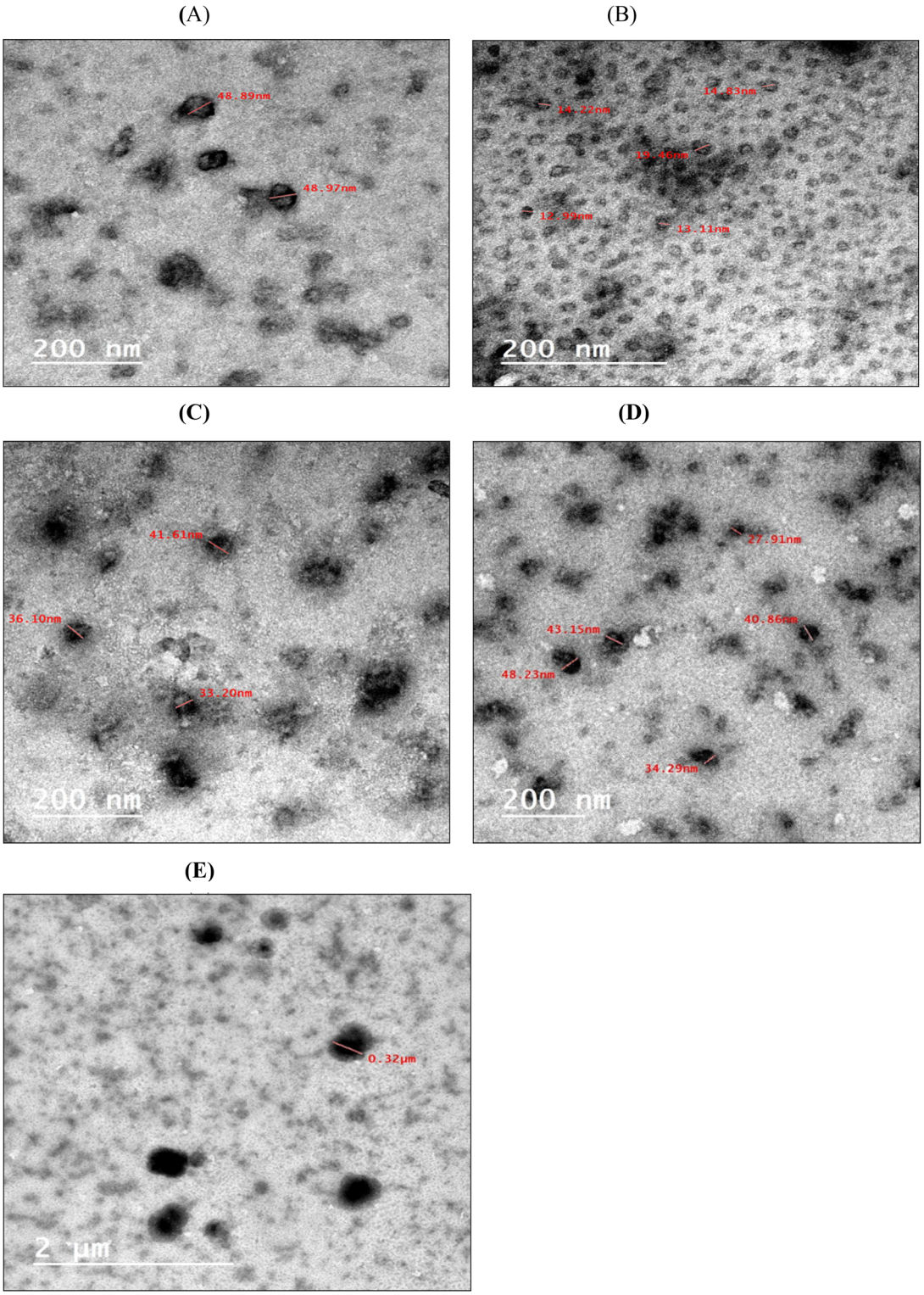

Fig. 2 Transmission electron micrographs of (A) linalool, (B) citral, (C) isoamyl acetate, (D) allyl caproate, and (E) orange peel oil nanoemulsions.

encapsulated in the same settings (Fig. 2E). This may have something to do with the Ostwald ripening phenomena, in which the oil phase of the emulsion system showed mild solubility in the surrounding aqueous phase with transfer from small to large droplets.[14]

3.2. Effect of flavorings and their nanoparticles on the nutritional parameters

In agreement with,[8] no changes could be observed in the initial or final body weights and meal efficiency (Table 3). The

Table 3 The impact of flavorings and their nanoparticles on nutritional parameters of the 8-week trial

Group	Initial body weight (g)	Final body weight (g)	Body gain (g)	Total food intake (g)	Feed Efficiency
Negative control	186.2 ± 3.35	215.7 ± 4.48	29.5 ± 1.13	7135.5 ± 3.29	0.004 ± 0.34
Positive control	185.4 ± 2.33^{a}	195.2 ± 3.87^{a}	9.8 ± 1.54^{a}	7100 ± 2.09^{a}	0.001 ± 0.74^{a}
Group (1)	184.9 ± 3.82^{a}	198.2 ± 4.35^{a}	13.3 ± 0.53^{b}	7130.5 ± 4.63^{b}	0.002 ± 0.11^{a}
Group (2)	185.8 ± 3.92^{a}	199.2 ± 4.35^{a}	13.4 ± 0.43^{c}	7120.2 ± 3.63^{c}	0.002 ± 0.12^{a}
Group (3)	184.2 ± 4.13^{a}	190.3 ± 4.67^{a}	6.1 ± 0.54^{d}	7125.8 ± 2.24^{d}	0.001 ± 0.24^{a}
Group (4)	184.2 ± 3.45^{a}	191.5 ± 3.55^{a}	7.3 ± 0.1^{e}	7115.5 ± 2.17^{e}	0.001 ± 0.05^{a}
Group (5)	185 ± 3.53^{a}	201.2 ± 4.87^{a}	16.2 ± 1.34^{f}	7123.2 ± 3.09^{f}	0.002 ± 0.43^{a}
Group (6)	184 ± 3.76^{a}	200.7 ± 3.97^{a}	16.7 ± 0.21^{g}	7125 ± 2.61^{g}	0.002 ± 0.08^{a}
Group (7)	183.8 ± 3.95^{a}	197.2 ± 4.35^{a}	13.4 ± 0.4^{h}	7130.2 ± 3.63^{h}	0.002 ± 0.11^{a}
Group (8)	182.9 ± 4.13^{a}	196.3 ± 4.67^{a}	13.8 ± 0.54^{i}	7127.3 ± 2.24^{i}	0.002 ± 0.24^{a}
Group (9)	182.5 ± 3.25^{a}	196.5 ± 3.5^{a}	14 ± 0.25^{j}	7122.5 ± 2.27^{j}	0.002 ± 0.11^{a}
Group (10)	182.3 ± 3.15^{a}	196.5 ± 5.5^{a}	14.2 ± 2.35^{k}	7123.5 ± 2.97^{k}	0.002 ± 0.79^{a}

Values were represented as mean ± SE (n = 6), in which the same letters in each column reflect a non-significant difference across varieties, whereas different letters reflect a significant difference at $P \leq 0.05$. Feed Efficiency = (Body Gain/Total Food Intake).

same pattern was studied by,[6] which showed the effect of D-limonene on streptozotocin-induced rats with a considerable reduction in body weight relative to the negative control rats. Table 3 shows that there are no significant differences in the initial and final body weights or feed efficiency in all groups compared to the negative and positive control groups. Meanwhile, a significant decrease was observed in the body weight growth in the positive control group and all treated groups compared to the negative control (Table 3). A more significant decrease was observed in treated groups 3 and 4, compared to the positive control group, in contrast to the remaining treated ones. The positive control group exhibited significantly decreased overall food intake compared to the negative control group and all other treated groups (Table 3). The decrease in body gain was observed in the positive control and treated groups due to structural proteins being lost or broken down in streptozotocin-induced diabetes, leading to a large body weight loss.[45,46] confirmed a decrease in overall food intake while applying the extracted dihydroxy gymnemic triacetate from *Gymnema sylvestre* on STZ-induced diabetic rats with lower blood sugar and cholesterol in the long-term therapy of diabetes. These changes may be caused by a decline in stomach health, which prompts the refusal of meals to lessen the strain on the gastrointestinal tract and acid secretion.

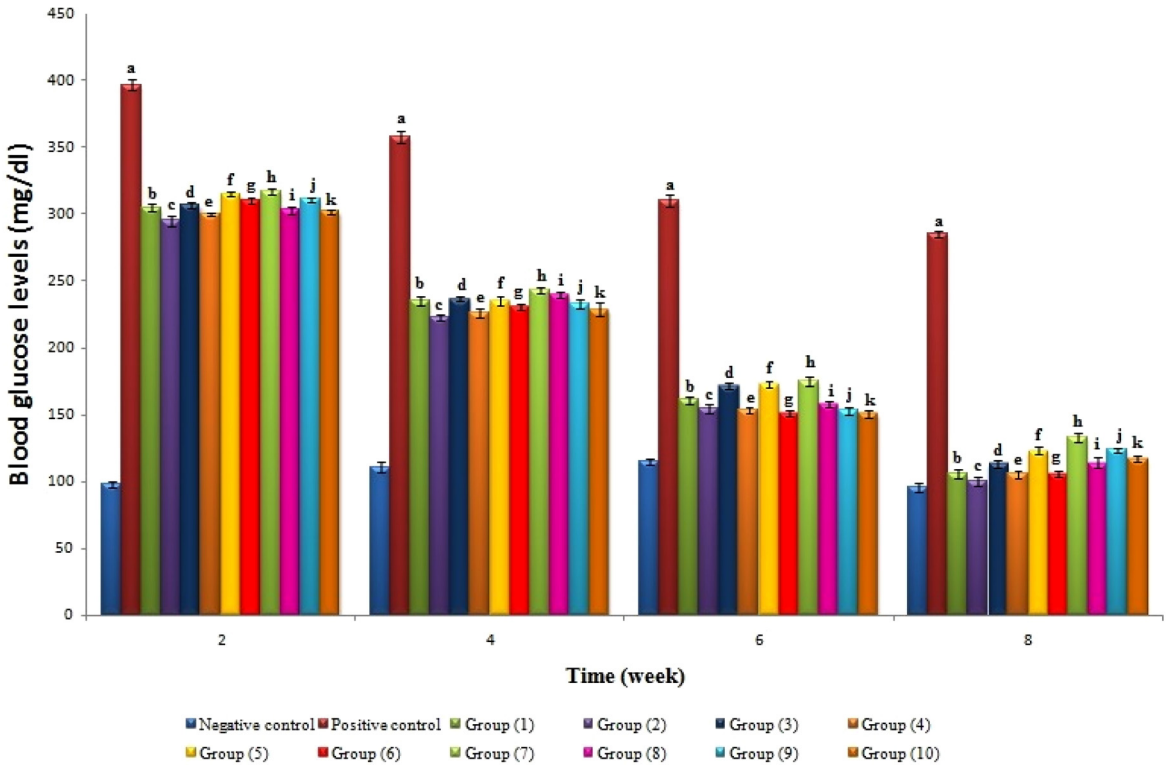

Fig. 3 Periodic changes in the blood glucose level.

3.3. Effect of nanoencapsulation forms on the biochemical parameters

Streptozotocin (STZ) is commonly used to create diabetes mellitus in experimental animals, which causes a reduction in insulin release.[47] It achieves this by triggering the degeneration and necrosis of the pancreatic islet of Langerhans cells. The mechanism of STZ is based on its glucose moiety, which can enter cells through the low-affinity glucose transporter GLUT2 in the plasma membrane. Then, STZ changes into reactive methyl carbonium ions that alkylate DNA and produce free radicals that target the DNA sugar moiety, breaking the DNA strand.[48] Blood glucose levels were monitored periodically every two weeks, as shown in Fig. 3. A significant decrease could be observed in all treated groups throughout the experimental period.

Table 4 shows that the positive control group had significantly higher levels of glucose, GHb%, TNF-α, and IL-6 than the negative control group. Interestingly, all treated groups exhibited significant decreases in the same metrics compared to the positive control group. The Hb level, which is regarded as a trustworthy indicator of diabetes, is inversely related to the fasting blood glucose levels, as reported by[49,50] in diabetic animals medicated with *Terminalia arjuna* and *Ferula duranii* extracts compared with positive control rats. TNF-α is a potent pro-inflammatory agent that affects many aspects of macrophage activity. It is rapidly released after trauma, infection, or exposure to bacterial-derived LPS, and is one of the early mediators that is most prevalent in inflamed tissue.[51] Therefore, the successful reduction of TNF-α in treated groups represents a potential target, as TNF-α has been proposed as a central player in inflammatory cell activation and the development of many chronic inflammatory diseases. A significant decrease in insulin level in the positive control group was observed compared to the negative control group. All treatment groups were caused by either damage or improper functioning of the β-cells. Nevertheless, all treated groups had higher insulin levels, showing they can stimulate β-cell regeneration or insulin production from these cells, which agreed with an earlier study[8] that confirmed the decreased blood

Table 4 Effect of flavorings and their nanoforms on the biochemical parameters

Group	Glucose (mg dL^{-1})	Insulin (μU ml^{-1})	GHb (%)	TNF-α (pg ml^{-1})	IL-6 (pg ml^{-1})	AST (U L^{-1})	ALT (U L^{-1})	ALP (U L^{-1})	Albumin (g L^{-1})	Total Protein (μmol L^{-1})
Negative control	95.7 ± 3.55	17.16 ± 2.13	5.1 ± 0.45	97.16 ± 5.13	48.1 ± 2.65	132.8 ± 1.71	94.6 ± 1.07	65.7 ± 3.19	2.78 ± 1.22	11.77 ± 0.54
Positive control	285.5 ± 2.34^{a}	9.51 ± 2.27^{a}	13.4 ± 0.31^{a}	218.5 ± 3.27^{a}	183.4 ± 3.31^{a}	240.5 ± 1.46^{a}	201.3 ± 2.37^{a}	115.1 ± 3.28^{a}	1.77 ± 1.17^{a}	6.28 ± 0.43^{a}
Group (1)	105.6 ± 3.43^{b}	14.3 ± 2.23^{b}	7.3 ± 0.25^{b}	115.3 ± 3.23^{b}	42.3 ± 3.25^{b}	127.5 ± 1.35^{b}	118.5 ± 2.32^{b}	71.1 ± 2.21^{b}	2.74 ± 2.29^{b}	12.62 ± 0.38^{b}
Group (2)	100± 3.35^{c}	13.16 ± 2.03^{c}	6.1 ± 0.45^{c}	114.19 ± 2.03^{c}	43.1 ± 3.45^{c}	120.7 ± 1.15^{c}	117.2 ± 3.18^{c}	69.3 ± 2.78^{c}	2.29 ± 2.16^{c}	11.83 ± 0.39^{c}
Group (3)	113.2 ± 2.44^{d}	13.61 ± 2.27^{d}	9.1 ± 0.31^{d}	116.61 ± 2.27^{d}	44.1 ± 2.31^{d}	137 ± 1.48^{d}	125.8 ± 1.33^{d}	83.5 ± 2.09^{d}	2.54 ± 1.13^{d}	13.17 ± 0.14^{d}
Group (4)	105.4 ± 3.23^{e}	12.3 ± 2.43^{e}	8.5 ± 0.25^{e}	115.3 ± 2.43^{e}	43.2 ± 2.25^{e}	128.2 ± 1.67^{e}	123.1 ± 2.67^{e}	80.78 ± 5.48^{e}	2.39 ± 1.17^{e}	12.38 ± 0.18^{e}
Group (5)	123.3± 3.35^{f}	11.16 ± 3.03^{f}	8.1 ± 0.45^{f}	115.16 ± 3.03^{f}	43.1 ± 2.45^{f}	147.5 ± 1.36^{f}	132.5 ± 2.32^{f}	75.4 ± 2.11^{f}	2.78 ± 2.32^{f}	13.47 ± 0.39^{f}
Group (6)	105.6 ± 2.44^{g}	10.61 ± 3.27^{g}	7.4 ± 0.31^{g}	114.61 ± 3.27^{g}	43.4 ± 2.51^{g}	139.7 ± 1.15^{g}	130.2 ± 2.58^{g}	71.5 ± 2.18^{g}	2.29 ± 2.17^{g}	12.98 ± 0.33^{g}
Group (7)	133.4 ± 3.23^{h}	12.3 ± 2.53^{h}	10.5 ± 0.25^{h}	116.13 ± 2.53^{h}	43.5 ± 2.25^{h}	157.2 ± 1.28^{h}	131.8 ± 1.53^{h}	88.1 ± 2.12^{h}	2.14 ± 1.19^{h}	13.12 ± 0.31^{h}
Group (8)	114.2± 3.75^{i}	10.16 ± 2.43^{i}	9.9 ± 0.45^{i}	115.76 ± 2.43^{i}	45.9 ± 2.45^{i}	148.1 ± 1.17^{i}	129.7 ± 2.67^{i}	80.7 ± 2.41^{i}	2.39 ± 1.22^{i}	12.63 ± 0.22^{i}
Group (9)	123.5 ± 2.14^{j}	10.61 ± 2.27^{j}	9.4 ± 0.31^{j}	116.71 ± 2.27^{j}	46.4 ± 2.31^{j}	135.5 ± 1.48^{j}	125.8 ± 2.83^{j}	76.3 ± 2.33^{j}	2.54 ± 2.13^{j}	13.57 ± 0.25^{j}
Group (10)	117.3 ± 2.43^{k}	10.3 ± 2.73^{k}	8.6 ± 0.25^{k}	115.5 ± 2.73^{k}	46.6 ± 2.25^{k}	130.2 ± 1.57^{k}	120.7 ± 2.67^{k}	70.8 ± 2.46^{k}	2.79 ± 2.16^{k}	12.78 ± 0.38^{k}

Values were represented as mean ± SE (n = 6), in which the same letters in each column reflect a non-significant difference across varieties, whereas different letters reflect a significant difference at $P \leq 0.05$.

Table 5 The effect of flavorings in nano-encapsulated forms on the total cholesterol, HDL, LDL, triglycerides, creatinine, urea, and uric acid

Group	Total cholesterol (mg dL^{-1})	HDL (mg dL^{-1})	LDL (mg dL^{-1})	Triglycerides (mg dL^{-1})	Creatinine (mg dL^{-1})	Urea (mg dL^{-1})	Uric Acid (mg dL^{-1})
Negative control	88.6 ± 3.45	47.7 ± 3.56	30.8 ± 2.61	48.5 ± 2.30	0.85 ± 0.03	35.4 ± 1.24	2.87 ± 0.14
Positive control	116.1 ± 3.6^{a}	32.1 ± 3.7^{a}	62.7 ± 3.26^{a}	65.8 ± 3.51^{a}	0.95 ± 0.04^{a}	38.6 ± 1.33^{a}	3.52 ± 0.28^{a}
Group (1)	88.2 ± 3.95^{b}	40.6 ± 1.35^{b}	30.3 ± 2.29^{b}	41.4 ± 3.64^{b}	0.86 ± 0.02^{b}	35.7 ± 1.13^{a}	2.73 ± 0.18^{b}
Group (2)	88.4± 3.24^{c}	45.1 ± 4.22^{c}	31.3 ± 2.87^{c}	40.7 ± 7.42^{c}	0.85 ± 0.02^{c}	35.9 ± 1.12^{a}	2.69 ± 0.15^{c}
Group (3)	89.3 ± 5.14^{d}	46.9 ± 0.97^{d}	31.2 ± 3.69^{d}	48.1 ± 7.05^{d}	0.88 ± 0.02^{d}	37.8 ± 2.57^{a}	2.80 ± 0.18^{d}
Group (4)	89 ± 2.45^{e}	45.8 ± 0.85^{e}	32.2 ± 1.88^{f}	47.9 ± 6.31^{e}	0.86 ± 0.04^{e}	37.9 ± 1.37^{a}	2.78 ± 0.19^{e}
Group (5)	101.5 ± 3.43^{f}	51.5 ± 1.56^{f}	31.9 ± 1.61^{f}	53.1 ± 5.30^{f}	0.90 ± 0.03^{f}	36.1 ± 1.04^{a}	2.77 ± 0.17^{f}
Group (6)	100.1 ± 2.6^{g}	52.1 ± 1.7^{g}	36.7 ± 2.26^{g}	52.8 ± 4.31^{g}	0.88 ± 0.04^{g}	36.2 ± 1.33^{a}	2.71 ± 0.18^{g}
Group (7)	93.6 ± 2.95^{h}	49.6 ± 1.35^{h}	33.3 ± 2.29^{h}	49.4 ± 6.64^{h}	0.89 ± 0.02^{h}	37.2 ± 1.13^{a}	2.75 ± 0.24^{h}
Group (8)	93.8 ± 4.04^{i}	50.1 ± 3.22^{i}	32.3 ± 2.87^{i}	48.7 ± 6.12^{i}	0.88 ± 0.03^{i}	37.5 ± 1.12^{a}	3.75 ± 0.25^{i}
Group (9)	96.2 ± 6.34^{j}	54.4 ± 0.97^{j}	33.2 ± 4.69^{j}	48.9 ± 7.25^{j}	0.90 ± 0.02^{j}	37.8 ± 2.57^{a}	2.76 ± 0.17^{j}
Group (10)	96.5 ± 6.45^{k}	54.8 ± 0.75^{k}	32.2 ± 1.88^{k}	48.1 ± 4.31^{k}	0.88 ± 0.03^{k}	37.9 ± 1.37^{a}	2.71 ± 0.19^{k}

Values were represented as Mean ± SE (n = 6), in which the same letters in each column reflect a non-significant difference across varieties, whereas different letters reflect a significant difference at $P \leq 0.05$.

glucose level and increased plasma insulin in diabetic rats due to supplemented diets with citral. Therefore, the anti-hyperglycemic activities of flavorings and their nanoparticles should be due to their effect on improving pancreatic β-cells function. Similarly, positive control and treated groups decrease the elevated levels of serum enzymes caused by STZ induction, as previously reported.[52]

The positive control group had significantly elevated serum enzyme levels (AST, ALT, and ALP) compared to the negative control group (Table 4). Different flavorings and their nano-

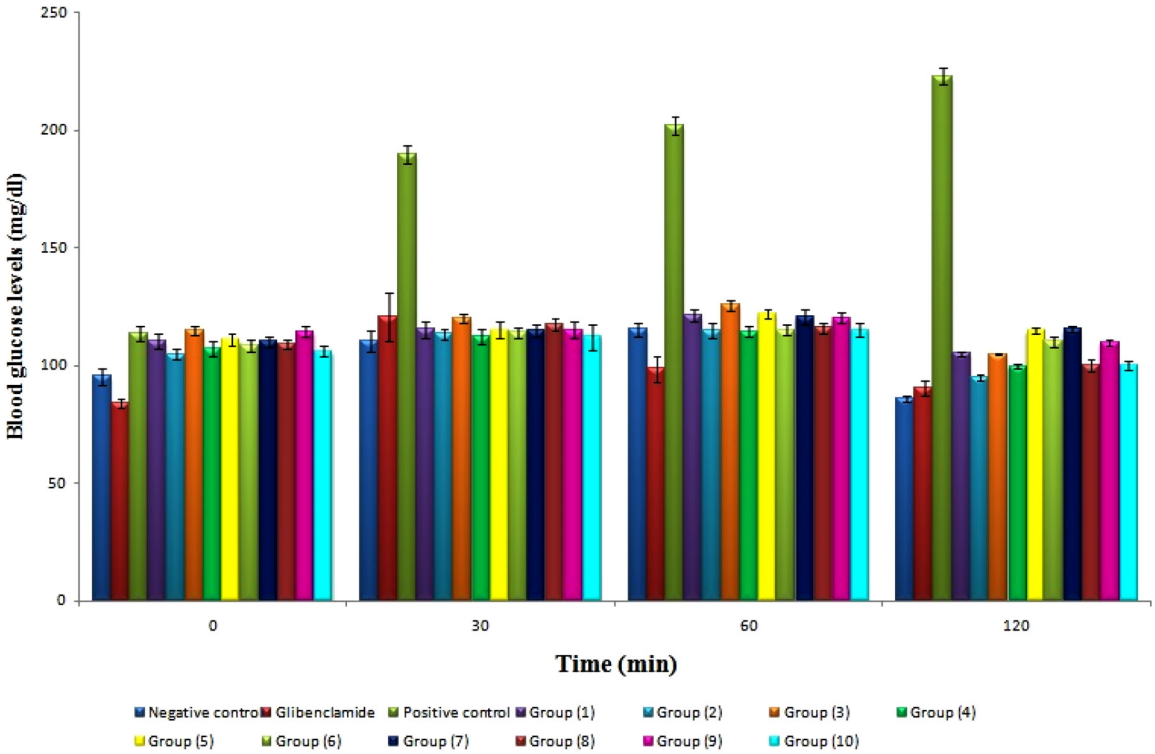

Fig. 4 Effect of flavorings and their nanocapsules on the oral glucose tolerance test (OGTT).

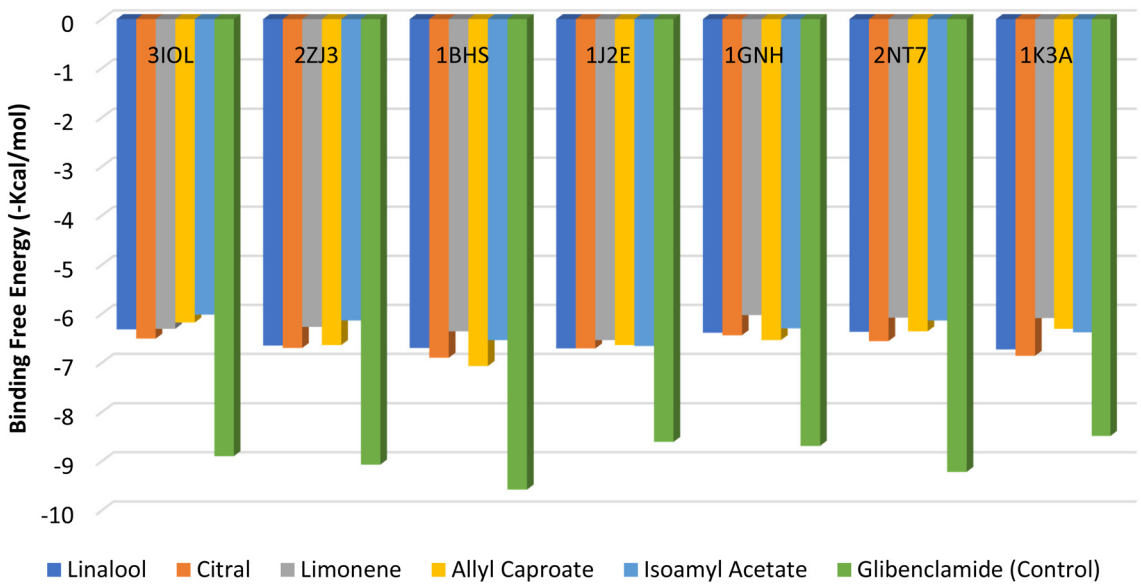

Fig. 5 Binding free energy values were calculated by molecular docking of the flavorings and receptors.

forms demonstrated pronounced protective effects *via* decreasing levels of serum enzymes altered by STZ induction (Table 4).

The significant reduction in albumin and total protein levels (Table 4) in the positive control compared to the negative control or treated groups with flavorings and their nanoforms is due to glycation of renal matrix proteins causing alterations in kidney architecture and increased basement membrane permeability, resulting in nephropathy.[53] These gradual alterations build up over time, eventually leading to renal failure. Preventing protein glycation can be very helpful in preventing the formation of such alterations. Microproteinuria and albuminuria, vital clinical indicators of diabetic nephropathy, and/or enhanced protein catabolism could explain the decrease in total protein and albumin percentage.[54]

Table 5 shows that the diabetic groups treated with flavorings and their nanoparticles decreased the serum lipid profile (total cholesterol, LDL, and triglycerides) compared to the positive control group. The findings show that the positive control group had significantly higher creatinine, urea, and uric acid levels than the negative control group. The lipid-lowering effect of the flavoring nanoparticle-treated groups (Table 5) might avoid cardiovascular disease in diabetes, which is supported by an increased serum insulin level in the treated groups, as summarized in Table 4. The previous findings agreed with,[55] where an aqueous extract of *Ocimum sanctum* L. leaves showed anti-hyperglycemic and lipid-lowering activities in the positive control group rats due to its effect on improving pancreatic β-cells function. It has been established that various metabolic and regulatory abnormalities that occur during diabetes lead to hyperlipidemic conditions

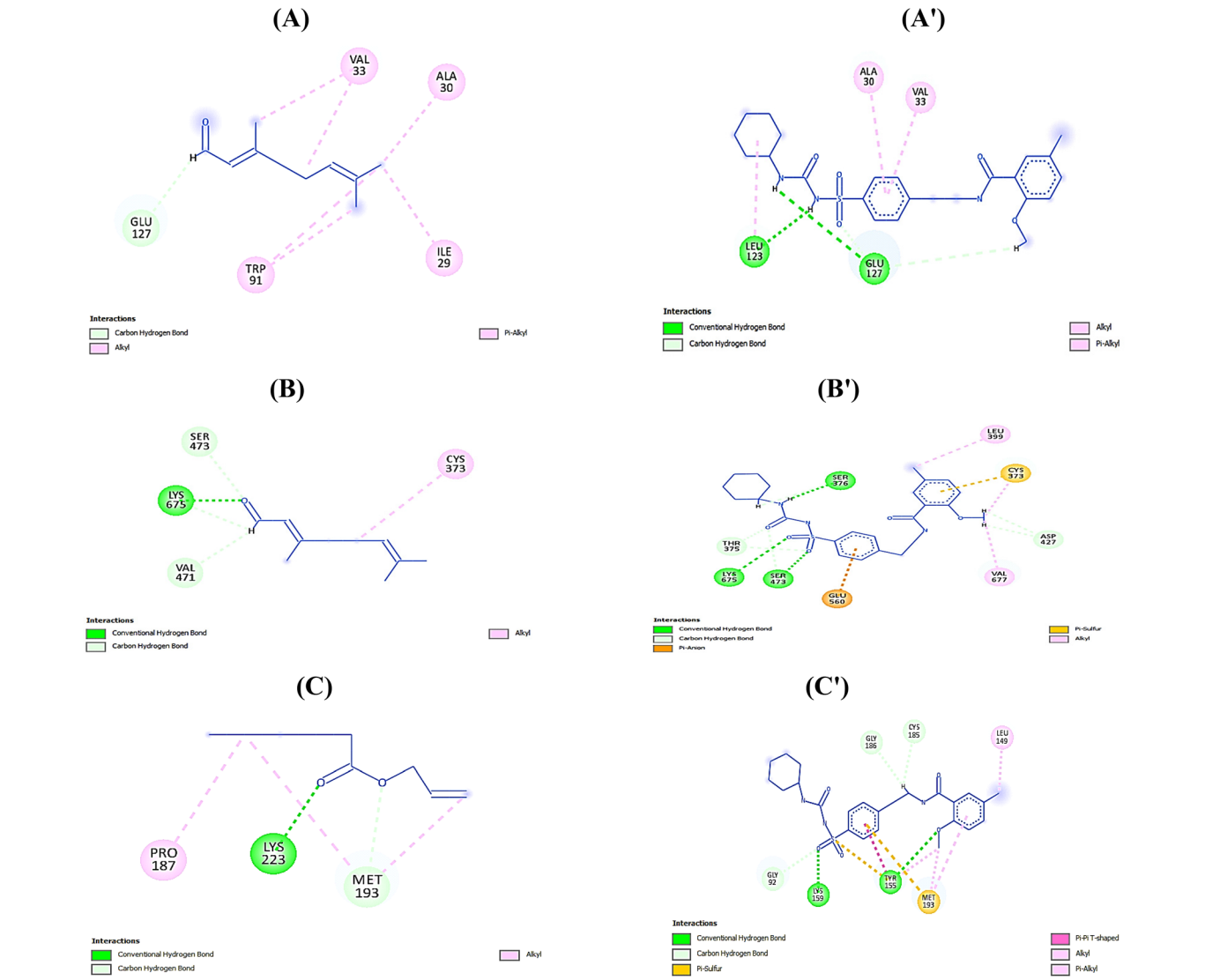

Fig. 6 Interactions of (A and A′) Citral and control with 3IOL, (B and B′) Citral and control with 2ZJ3, (C and C′) Allyl caproate and control with 1BHS, (D and D′) linalool and control with 1J2E, (E, E′) Allyl caproate and control with 1GNH, (F and F′) Citral and control with 2NT7, and (G and G′) Citral and control with 1K3A.

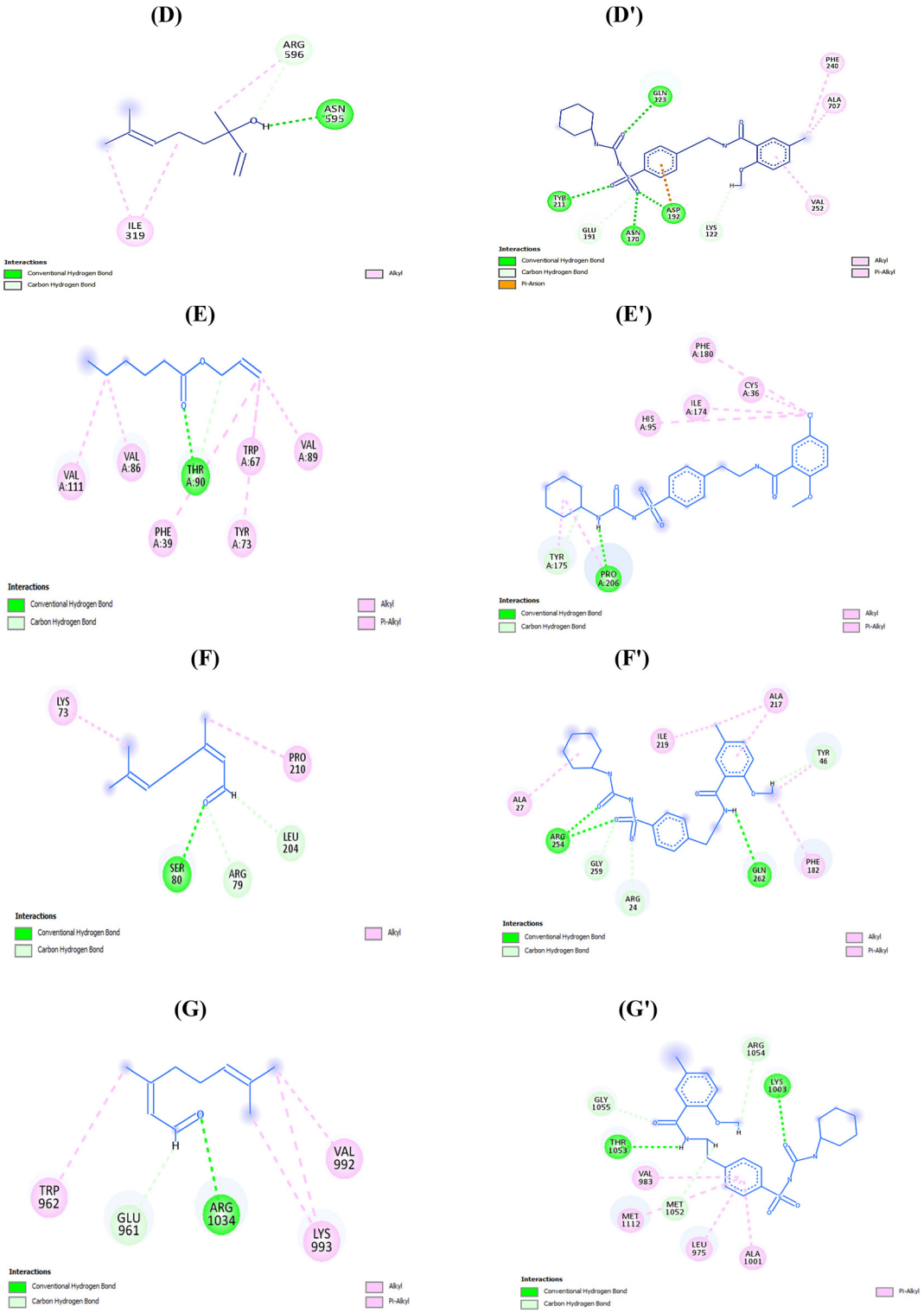

Fig. 6 *(Contd).*

in people with diabetes, while increased TC, LDL-C, and TG levels in the blood cause diabetic dyslipidemia.[56,57]

The findings show that the positive control group had significantly higher creatinine, urea, and uric acid levels than the negative control group. All treated groups had significantly lower creatinine, urea, and uric acid levels than the positive control group, which is in line with the negative control group (Table 5). It was revealed that circulating lipids bind to and become trapped by the extracellular matrix, where they are oxidized, increasing the reactive oxygen species generation, which

could damage the structure and function of diabetic kidneys.[58] Therefore, treatment with flavorings in nano-encapsulated and non-encapsulated forms inhibited lipid alterations, which could be one explanation for its possible renoprotective activity.

The oral glucose tolerance test (OGTT) assesses insulin resistance and apparent insulin release in many clinical settings. The blood samples for the OGTT were examined for glucose content at 0, 30, 60, and 120 minutes, respectively (Fig. 4). Citral, linalool, allyl caproate, isoamyl acetate, and orange oil in raw and nano-encapsulated forms showed no discernible hypoglycemia effects in normal rats. The current study is based on Glibenclamide, a long-used positive control used to treat diabetes and promote insulin secretion. The blood glucose levels of all treated groups had a significant with negative control and Glibenclamide at 30, 60 and 120 min. Based on the effect of flavorings and their nanoparticles on OGTT (Fig. 4), it is suggested that food flavorings such as citral, linalool, allyl caproate, isoamyl acetate, and orange oil in typical and nano-encapsulated forms may have insulin-mimetic activity. Further studies are necessary to reveal the mechanism of their action and the possibility of using them safely for T2DM patients. The previous findings agreed with,[6,8] which suggested the potential antihyperglycemic activity of limonene and citral in their original forms in streptozotocin-induced diabetic rats.

Flavorings in nanoforms showed lower levels of glucose and OGTT than those in free forms, as shown in Table 4 and Fig. 4. The previous findings agreed with many previous studies dealing with the effect of nanoparticles based upon inartificial polymers on STZ-induced diabetic rats. For example, due to chitosan's remarkable capacity to momentarily relax the tight junctions between epithelial cells and improve adhesion to negatively charged mucosal surfaces, ferulic acid-chitosan nanoparticles demonstrated an *in vivo* oral bioavailability that was four times greater than that of free ferulic acid. This resulted in a greater uptake of cells.[59] Similarly, a chitosan-alginate complex-prepared curcumin nanoformulation demonstrated a 30% greater glucose-lowering impact *in vivo* than chitosan alone.[60] Additionally,[61] created thymoquinone-loaded gum rosin nanocapsules with a greater antihyperglycemic effect in T2DM rats despite only having half as much administered as native thymoquinone.

3.4. Evaluation of molecular docking

Fig. 5 shows the binding capacity of the food flavorings under investigation: linalool, citral, limonene (which is the predominant orange peel oil), allyl caproate, isoamyl acetate, and Glibenclamide as a control on seven proteins related to T2DM. Binding energy values for the flavorings ranged from −6.02 to −7.07 kcal mol^{-1}. In this range, the highest scores were −6.51 to −7.07 kcal mol^{-1} for citral, linalool, and allyl caproate against the receptors. Therefore, they were selected for molecular docking demonstration, which is shown later in Fig. 5. However, the investigated flavorings showed a lower binding capacity than the control; Glibenclamide showed a binding energy range of −8.49 to −9.54 kcal mol^{-1}. The lower binding energy is due to the simple structure of the flavorings applied with a lack of aromaticity and few hydroxyls or other functional groups outside, which may explain their low binding affinity. Consequently, these compounds have a small tendency to develop a complex with the four target proteins.[62]

Fig. 6A–G shows the interaction of flavorings with the highest binding energy scores and the control (Glibenclamide) against five receptors. The higher binding affinity of the control with the 3IOL receptor compared to citral is attributed to the crucial conventional H-bonds formed with GLU127 and C–H interaction with LEU123. Citral is also connected to GLU127 through the C–H bond, and has similar alkyl interaction and pi-alkyl with ALA30 and VAL33 compared with the control (Fig. 6A and A′). Conventional hydrogen interactions firmly bind the control with the 2ZJ3 receptor residues SER376 and SER473, while bonding with the LYS675 moiety was common for both citral and the control against the 2ZJ3 receptor (Fig. 6B and, B′). The number, types, and uniqueness of bonds were the main criteria that led to the control's higher binding affinity with all investigated receptors contrasted with the highest flavorings, as shown in Fig. 4A′–G′. For example, allyl caproate showed a conventional H-bond with LYS223, C–H, and alkyl interaction with MET193 and PRO187 residues of the 1BHS receptor. On the other hand, the control showed more conventional H-bonding with the TYR155 and LYS159 moieties in addition to the C–H bonds (GLY186, CYS185, GLY92), pi-pi T-shaped (TYR155), pi-sulfur interaction (MET193, TYR155), and many other alkyls and pi-alkyl interactions with the same receptor (Fig. 6C and C′). In the same context, linalool, allyl caproate, and citral showed the same types and numbers of bonds with the moieties of the 1J2E, 1GNH, 2NTF, and 1K3A proteins (Fig. 6D–G), which revealed that the comparable binding energies values ranged from −6.54 to −6.86 kcal mol^{-1} (Fig. 5). The interactions between the moieties of the proteins involved in T2DM pathogenesis and flavorings agree with,[5] who reported similar molecular interactions between phenolic metabolites of black beans and blue corn extracts and the same protein moieties identified in the present study.

4. Conclusions

The current study examined the effect of food flavorings and their nanocapsules, which are widely used to increase food and pharmaceutical palatability, on T2DM patients. Using high-shear homogenization to encapsulate flavorings did not affect the volatile constituents of delivery systems with a higher encapsulation efficiency with the nanometric scales, as proved by both dynamic light scattering and transmission electron microscope techniques. Interestingly, nanoforms showed better results compared to raw flavorings. T2D rats treated with flavorings and their nanoparticles exhibited enhanced biochemical parameters and lowered glucose and OGTT levels. Thus, the flavorings used and their nanoformulations have the

potential double effect of a flavor compound as a food palatability enhancer with a potential beneficial effect on type 2 diabetes mellitus.

Author contributions

DMM: conceptualization, investigation, formal analysis, methodology, interpretation of biological data, statistical analysis, data curation and writing – software review & editing. AF: conceptualization, project administration, investigation, writing—original draft, methodology, formal analysis, statistical analysis, data curation, software and docking, revision and editing. MAA, MMG, ME: revision and editing. WAM, SA, HAE, MMG, ME: funding acquisition. All authors provided comments on the draft manuscript and approved the final version.

Conflicts of interest

There are no conflicts of interest to declare.

Acknowledgements

The authors are thankful to the Researchers Supporting project number (RSP2023R516) at King Saud University, Riyadh, Saudi Arabia, and to the Princess Nourah bint Abdulrahman University Researchers Supporting project number (PNURSP2023R171), Princess Nourah bint Abdulrahman University, Riyadh, Saudi Arabia.

References

1 H. A. E. Shaaban, A. H. El-Ghorab and T. Shibamoto, Bioactivity of essential oils and their volatile aroma components: Review, *J. Essent. Oil-Bear. Plants*, 2012, **24**, 203–212.

2 K. Mellendick, L. Shanahan, L. Wideman, S. Calkins, S. Keane and C. Lovelady, Diets rich in fruits and vegetables are associated with lower cardiovascular disease risk in adolescents, *Nutrients*, 2018, **10**, 136.

3 American Diabetes Association, Diagnosis and classification of diabetes mellitus, *Diabetes Care*, 2009, **32**, S62–S67.

4 K. Ogurtsova, L. Guariguata, N. C. Barengo, P. L. D. Ruiz, J. W. Sacre, S. Karuranga, H. Sun, E. J. Boyko and D. J. Magliano, IDF diabetes Atlas: Global estimates of undiagnosed diabetes in adults for 2021, *Diabetes Res. Clin. Pract.*, 2022, **183**, 109118.

5 K. Damián-Medina, Y. Salinas-Moreno, D. Milenkovic, L. Figueroa-Yáñez, E. Marino-Marmolejo, I. Higuera-Ciapara, A. Vallejo-Cardona and E. Lugo-Cervantes, In silico analysis of antidiabetic potential of phenolic compounds from blue corn (Zea mays L.) and black bean (Phaseolus vulgaris L.), *Heliyon*, 2020, **6**, e03632.

6 R. Murali and R. Saravanan, Antidiabetic effect of d-limonene, a monoterpene in streptozotocin-induced diabetic rats, *Biomed. Prev. Nutr.*, 2012, **2**, 269–275.

7 T. A. More, B. R. Kulkarni, M. L. Nalawade and A. U. Arvindekar, Antidiabetic activity of linalool and limonene in streptozotocin-induced diabetic rat: a combinatorial therapy approach, *Int. J. Pharmacol. Pharm. Sci.*, 2014, **6**, 159–163.

8 C. Mishra, M. A. Khalid, N. Fatima, B. Singh, D. Tripathi, M. Waseem and A. A. Mahdi, Effects of citral on oxidative stress and hepatic key enzymes of glucose metabolism in streptozotocin/high-fat-diet induced diabetic dyslipidemic rats, *Iran. J. Basic Med. Sci.*, 2019, **22**, 49.

9 V. Manimaran, P. M. Sivakumar, J. Narayanan, S. Parthasarathi and P. K. Prabhakar, Nanoemulsions: A Better Approach for Antidiabetic Drug Delivery, *Curr. Diabetes Rev.*, 2021, **17**, 486–495.

10 S. Moawad, M. El-Kalyoubi, M. Khallaf, M. A. Abd El Mageed, H. Ali and A. Farouk, Influence of Carriers on the Functional Properties of Spray-Dried Flavors During Storage, *Egypt. J. Food Sci.*, 2021, **49**, 231–238.

11 J. Charve and G. A. Reineccius, Encapsulation performance of proteins and traditional materials for spray dried flavors, *J. Agric. Food Chem.*, 2009, **57**, 2486–2492.

12 S. Bouaouina, A. Aouf, A. Touati, H. Ali, M. Elkhadragy, H. Yehia and A. Farouk, Effect of Nanoencapsulation on the Antimicrobial and Antibiofilm Activities of Algerian Origanum glandulosum Desf. Against Multidrug-Resistant Clinical Isolates, *Nanomaterials*, 2022, **12**, 2630.

13 Z. Zhao, X. Cui, X. Ma and Z. Wang, Preparation, characterization, and evaluation of antioxidant activity and bioavailability of a self-nanoemulsifying drug delivery system (SNEDDS) for buckwheat flavonoids, *Acta Biochim. Biophys. Sin.*, 2020, **52**, 1265–1274.

14 H. Ali, A. R. Al-Khalifa, A. Aouf, H. Boukhebti and A. Farouk, Effect of nanoencapsulation on volatile constituents, and antioxidant and anticancer activities of Algerian *Origanum glandulosum* Desf. essential oil, *Sci. Rep*, 2020, **10**, 2812.

15 R. Adams, Identification of Essential Oil Components by Gas, in *Chromatography/Mass Spectroscopy*, Allured PublishingCorporation, Carol Stream, IL, USA, 4th edn, 2007.

16 AOAC, *Official Methods of Analysis of AOAC International*, AOAC International, Gaithersburg, MD, USA, 15th edn, 2009.

17 D. M. Mohammed, K. A. Ahmed, M. A. Desoukey and B. A. Sabry, Assessment of the antiulcer properties of Lawsonia inermis L. leaves and its nano-formulation against prolonged effect of acute ulcer in rats, *Toxicol. Rep.*, 2022, **9**, 337–345.

18 P. G. Reeves, F. H. Nielsen and G. C. Fahey Jr., AIN-93 purified diets for laboratory rodents: final report of the American Institute of Nutrition ad hoc writing committee on the reformulation of the AIN-76A rodent diet, *J. Nutr.*, 1993, **123**(11), 1939–1951.

19 D. M. Mohammed, N. Elsayed, D. H. Abou Baker, K. A. Ahmed and B. A. Sabry, Bioactivity and antidiabetic properties of Malva parviflora L. leaves extract and its nano-formulation in streptozotocin-induced diabetic rats, *Heliyon*, 2022, **8**, e12027.

20 B. Deepa and C. V. Anuradha, Linalool, a plant derived monoterpene alcohol, rescues kidney from diabetes-induced nephropathic changes via blood glucose reduction, *Diabetol. Croat.*, 2011, **40**, 121–138.

21 S. A. Clode, K. R. Butterworth, I. F. Gaunt, P. Grasso and S. D. Gangolli, Short-term toxicity study of allyl caproate in rats, *Food Cosmet. Toxicol.*, 1976, **16**, 197–201.

22 D. L. J. Opdyke, Monographs on fragrance raw materials, *Food Cosmet. Toxicol.*, 1975, **13**, 449–457.

23 D. V. Sweet, V. P. Anderson and J. C. F. Fang, An overview of the Registry of Toxic Effects of Chemical Substances (RTECS): Critical information on chemical hazards, *Chem. Health Saf.*, 1999, **6**, 12–16.

24 S. M. Cohen, G. Eisenbrand, S. Fukushima, N. J. Gooderham, F. P. Guengerich, S. S. Hecht, I. M. C. M. Rietjens, M. Bastaki, J. M. Davidsen, C. L. Harman, M. McGowen and S. V. Taylor, FEMA GRAS assessment of natural flavor complexes: Citrus-derived flavoring ingredients, *Food Cosmet. Toxicol.*, 2019, **124**, 192–218.

25 P. Trinder, Determination of glucose in blood using glucose oxidase with an alternative oxygen acceptor, *Ann. Clin. Biochem.*, 1969, **6**, 24–27.

26 D. L. Drabkin and J. H. Austin, Spectrophotometric studies: I. Spectrophotometric constants for common hemoglobin derivatives in human, dog, and rabbit blood, *J. Biol. Chem.*, 1932, **98**, 719–733.

27 W. Richmond, Preparation and properties of a cholesterol oxidase from Nocardia sp. and its application to the enzymatic assay of total cholesterol in serum, *Clin. Chem.*, 1973, **19**, 1350–1356.

28 C. C. Allain, L. S. Poon, C. S. Chan, W. F. P. C. Richmond and P. C. Fu, Enzymatic determination of total serum cholesterol, *Clin. Chem.*, 1974, **20**, 470–475.

29 M. F. Lopes-Virella, P. Stone, S. Ellis and J. A. Colwell, Cholesterol determination in high-density lipoproteins separated by three different methods, *Clin. Chem.*, 1977, **23**, 882–884.

30 H. Wieland and D. A. Seidel, Simple specific method for precipitation of low density lipoproteins, *J. Lipid Res.*, 1983, **24**, 904–909.

31 S. Reitman and S. Frankel, A Colorimetric method for the determination of serum glutamic oxalacetic and glutamic pyruvic transaminases, *Am. J. Clin. Pathol.*, 1957, **28**(1), 56–63.

32 A. L. Babson, S. J. Greeley, C. M. Coleman and G. E. Phillips, Phenolphthalein monophosphate as a substrate for serum alkaline phosphatase, *Clin. Chem.*, 1966, **12**, 482–490.

33 J. G. Rheinhold, Total protein, albumin and globulin, *Stand. Methods Clin. Chem.*, 1953, **1**, 88.

34 B. T. Doumas, W. A. Watson and H. G. Biggs, Albumin standards and the measurement of serum albumin with bromcresol green, *Clin. Chim. Acta*, 1971, **31**, 87–96.

35 J. Fawcett and J. A. Scott, Rapid and precise method for the determination of urea, *J. Clin. Pathol.*, 1960, **13**, 156–159.

36 J. Schirmeister, Determination of creatinine level, *Dtsch. Med. Wschr*, 1964, **89**, 1940–1947.

37 D. Barham and P. Trinder, An improved colour reagent for the determination of blood glucose by the oxidase system, *Analyst*, 1972, **97**, 142–145.

38 M. D. Hanwell, D. E. Curtis, D. C. Lonie, T. Vandermeersch, E. Zurek and G. R. Hutchison, Avogadro: an advanced semantic chemical editor, visualization, and analysis platform, *J. Cheminf.*, 2012, **4**, 1–17.

39 A. Aouf, S. Bouaouina, M. A. Abdelgawad, M. A. S. Abourehab and A. Farouk, In Silico Study for Algerian Essential Oils as Antimicrobial Agents against Multidrug-Resistant Bacteria Isolated from Pus Samples, *Antibiotics*, 2022, **11**, 1317.

40 A. Farouk, A. S. Hathout, M. M. Amer, O. A. Hussain and S. Fouzy, The Impact of Nanoencapsulation on Volatile Constituents of Citrus sinesis L. Essential Oil and their Antifungal Activity, *Egypt. J. Chem.*, 2022, **65**, 527–538.

41 J. Y. Min, S. I. Ahn, Y. K. Lee, H. S. Kwak and Y. H. Chang, Optimized conditions to produce water-in-oil-in-water nanoemulsion and spray-dried nanocapsule of red ginseng extract, *Food Sci. Technol*, 2018, **38**, 485–492.

42 S. Roshanpour, J. Tavakoli, F. Beigmohammadi and S. Alaei, Improving antioxidant effect of phenolic extract of Mentha piperita using nanoencapsulation process, *J. Food Meas. Charact.*, 2021, **15**, 23–32.

43 R. Lutz, A. Aserin, L. Wicker and N. Garti, Release of electrolytes from W/O/W double emulsions stabilized by a soluble complex of modified pectin and whey protein isolate, *Colloids Surf., B*, 2009, **74**, 178–185.

44 V. Klang, N. B. Matsko, C. Valenta and F. Hofer, Electron microscopy of nanoemulsions: An essential tool for characterization and stability assessment, *Micron*, 2012, **43**, 85–103.

45 B. Raghavan and S. K. Kumari, Effect of Terminalia arjuna stem bark on antioxidant status in liver and kidney of alloxan diabetic rats, *Indian J. Physiol. Pharmacol.*, 2006, **50**, 133.

46 P. Daisy, J. Eliza and K. A. M. M. Farook, A novel dihydroxy gymnemic triacetate isolated from Gymnema sylvestre possessing normoglycemic and hypolipidemic activity on STZ-induced diabetic rats, *J. Ethnopharmacol.*, 2009, **126**, 339–344.

47 N. T. Faqih, A. F. Ashoor, S. A. Alshaikh, A. F. Maglan and N. Jastaniah, Association of Alzheimer's Disease and Insulin Resistance in King Abdulaziz Medical City, Jeddah, *Cureus*, 2021, **13**, e19811.

48 M. Elsner, B. Guldbakke, M. Tiedge, R. Munday and S. Lenzen, Relative importance of transport and alkylation for pancreatic beta-cell toxicity of streptozotocin, *Diabetologia*, 2000, **43**, 1528–1533.

49 K. Parveen, R. Khan and W. A. Siddiqui, Antidiabetic effects afforded by Terminalia arjuna in high fat-fed and streptozotocin-induced type 2 diabetic rats, *Int. J. Diabetes Metab.*, 2011, **19**, 23–33.
50 H. S. Yusufoglu, G. A. Soliman, R. F. Abdel-Rahman, M. S. Abdel-Kader, M. A. Ganaie, E. Bedir, S. Baykan and B. Ozturk, Antihyperglycemic and antihyperlipidemic effects of Ferula duranii in experimental type 2 diabetic rats, *Int. J. Clin. Pharmacol.*, 2015, **11**, 532–541.
51 G. L. King, The role of inflammatory cytokines in diabetes and its complications, *J. Periodontol.*, 2008, **79**, 1527–1534.
52 S. P. Panda, P. K. Haldar, S. Bera, S. Adhikary and C. C. Kandar, Antidiabetic and antioxidant activity of Swietenia mahagoni in streptozotocin-induced diabetic rats, *Pharm. Biol.*, 2010, **48**, 974–979.
53 J. M. Forbes, M. E. Cooper, M. D. Oldfield and M. C. Thomas, Role of advanced glycation end products in diabetic nephropathy, *J. Am. Soc. Nephrol.*, 2003, **14**(suppl 3), S254–S258.
54 G. L. Bakris, A. Mangrum, J. B. Copley, N. Vicknair and R. Sadler, Effect of calcium channel or β-blockade on the progression of diabetic nephropathy in African Americans, *Hypertension*, 1997, **29**, 744–750.
55 T. Suanarunsawat, W. D. N. Ayutthaya, S. Thirawarapan and S. Poungshompoo, Anti-oxidative, anti-hyperglycemic and lipid-lowering effects of aqueous extracts of Ocimum sanctum L. leaves in diabetic rats, *Food Sci. Nutr.*, 2014, **5**, 801–811.
56 I. Raz, R. Eldor, S. Cernea and E. Shafrir, Diabetes: insulin resistance and derangements in lipid metabolism. Cure through intervention in fat transport and storage, *Diabetes/Metab. Res. Rev.*, 2005, **21**, 3–14.
57 D. H. Abou Baker and D. M. Mohammed, Polyphenolic rich fraction of Physalis peruviana calyces and its nano emulsion induce apoptosis by caspase 3 up-regulation and G2/M arrest in hepatocellular carcinoma, *Food Biosci.*, 2022, **50**, 102007.
58 R. Trevisan, A. R. Dodesini and G. Lepore, Lipids and renal disease, *J. Am. Soc. Nephrol.*, 2006, **17**(4 suppl 2), S145–S147.
59 R. Panwar, N. Raghuwanshi, A. K. Srivastava, A. K. Sharma and V. Pruthi, *In vivo* sustained release of nanoencapsulated ferulic acid and its impact in induced diabetes, *Mater. Sci. Eng., C*, 2018, **92**, 381–339.
60 J. O. Akolade, H. O. B. Oloyede and P. C. Onyenekwe, Encapsulation in chitosan-based polyelectrolyte complexes enhances antidiabetic activity of curcumin, *J. Funct. Foods*, 2017, **35**, 584–594.
61 R. Rani, S. Dahiya, D. Dhingra, N. Dilbaghi, K. H. Kim and S. Kumar, Improvement of antihyperglycemic activity of nano-thymoquinone in rat model of type-2 diabetes, *Chem.-Biol. Interact.*, 2018, **295**, 119–132.
62 T. H. Nguyen Vo, N. Tran, D. Nguyen and L. Le, An in silico study on antidiabetic activity of bioactive compounds in Euphorbia thymifolia Linn, *SpringerPlus*, 2016, **5**, 1–13.